



Cite this: *Phys. Chem. Chem. Phys.*, 2025, 27, 5949

Received 22nd January 2025,
Accepted 23rd February 2025

DOI: 10.1039/d5cp00303b

rsc.li/pccp

An archetype of hydrogen bonding observed in cationic dimers of carboxy-functionalized ionic liquids by means of NMR solid state spectroscopy – reminiscent of salt bridges, peptides and DNA[†]

Alexander E. Khudozhitkov,^{id ae} Lasse Hunger,^b Loai Al-Sheakh,^b Alexander G. Stepanov,^{id a} Daniil I. Kolokolov^{id *ae} and Ralf Ludwig^{id *bcd}

Ion pair formation is a fundamental concept in chemistry. The association between ions of opposite charge is widely used in synthesis and catalysis. In contrast, there is little evidence for the formation of cationic or anionic dimers in solution. We report the strength and distribution of doubly hydrogen bonded cationic dimers ($c^+ = c^+$) in carboxy-functionalized ionic liquids [$\text{HOOC-(CH}_2\text{)}_n\text{-py}[NTf}_2\text{]$ with $n = 2, 4, 5, 6, 7$, and 9 , probed by NMR solid-state spectroscopy. The two $\text{OH} \cdots \text{O}=\text{C}$ H-bonds of the cationic dimers resemble the archetype H-bond motif known for formic acid. Herein, we clarify how the propensity for the formation of ($c^+ = c^+$) H-bonds depends on the alkyl chain length between the pyridinium ring and the carboxy group of the cations. For $n = 9$, the H-bond population is primarily dominated by cationic dimers ($c^+ = c^+$). Obviously, cooperative H-bond attraction is not only able to compensate for the repulsive Coulomb forces but also to ignore the H-bond accepting capabilities of the counter anion completely. In this regard, we provide the first evidence for quasi-isolated cationic dimers in solution that are stabilized by strong and directional ($c^+ = c^+$) H-bonds being as strong as the ($m=m$) H-bonds between molecular mimics of the IL cations.

Introduction

Hydrogen bonds are ubiquitous in nature and of fundamental importance for the liquid and solid structure of water as well as

for the stability and function of proteins and DNA.¹ The base pairs in double-stranded DNA are held together by double and triple hydrogen bonds (H-bonds), protecting it from disruption.² In order to understand the fundamental properties of these multiple H-bonds, the dimers of formic acid and acetic acid in the liquid and gaseous state became the focus of intensive research. The H-bond energy of these archetypes of binding motif ranges between 60 and 70 kJ mol^{-1} .³⁻⁶ Due to cooperation effects, the two H-bonds are stronger than the double of the individual H-bonds. Here, most H-bonds pair up two neutral molecules. However, there are also a range of systems where one or the other species is electrically charged such as zwitterions in peptides.⁷ This is in particular true for ionic liquids, which consist solely of cations and anions.⁸⁻¹¹ Therein, we usually find a cation proton donor and an anion acceptor. Thus, H-bonds are charge-assisted following the conventional wisdom that opposite charges attract, but like charges repel. The question has arisen as to whether a pair of molecules can engage in an attractive H-bond if both entities are of like charge, despite the chemical intuition that two subunits ought to strongly repel one another. Theoretical studies showed that the paired complexes of like charged ions are higher in energy than those of the isolated ions but create a shallow local minimum on the surface.¹²⁻¹⁶ The most stable pair of cations could be calculated for a pair of carboxylic acids, each containing a cationic NH_3^+ tail. A pair of two equivalent H-bonds of type $\text{OH} \cdots \text{O}$ hold this dimer together with $\text{R}(\text{H} \cdots \text{O})$ at 1.962 \AA .¹³ The presence of true H-bonds is confirmed by the geometry and NMR ^1H chemical shifts. Recently, we succeeded in realizing such a scenario in carboxy-functionalized ionic liquids (ILs). We synthesized ILs [$\text{HOOC-(CH}_2\text{)}_n\text{-py}[NTf}_2\text{]$] with varying number of methylene groups CH_2 ($n = 1, 2, 4$) for distancing the carboxy group COOH from the positively charged pyridinium ring as shown in Scheme 1. This way, the repulsive Coulombic forces were reduced and the two H-bonds $\text{OH} \cdots \text{O}$ between the cations could be strongly enhanced.¹⁷ This archetype structural motif of acetic dimers was observed in the

^a Boreskov Institute of Catalysis, Siberian Branch of Russian Academy of Sciences, Prospekt Akademika Lavrentieva 5, Novosibirsk, 630090, Russia.

E-mail: kdi@catalysis.ru

^b Universität Rostock, Institut für Chemie, Abteilung für Physikalische Chemie, Dr-Lorenz-Weg 2, Rostock 18059, Germany. E-mail: ralf.ludwig@uni-rostock.de; Tel: +49 381 498 6517

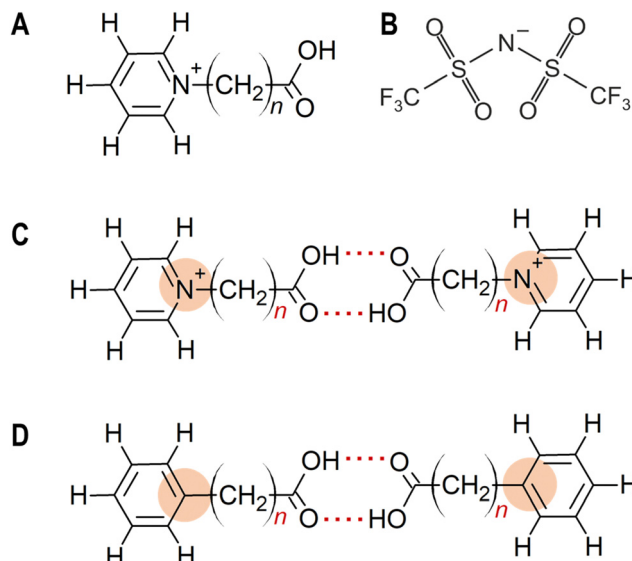
^c Department LL&M, University of Rostock, Albert-Einstein-Str. 25, Rostock 18059, Germany

^d Leibniz-Institut für Katalyse an der Universität Rostock e.V., Albert-Einstein-Str. 29a, Rostock 18059, Germany

^e Novosibirsk State University, Pirogova Street 2, Novosibirsk, 630090, Russia

[†] Electronic supplementary information (ESI) available. See DOI: <https://doi.org/10.1039/d5cp00303b>





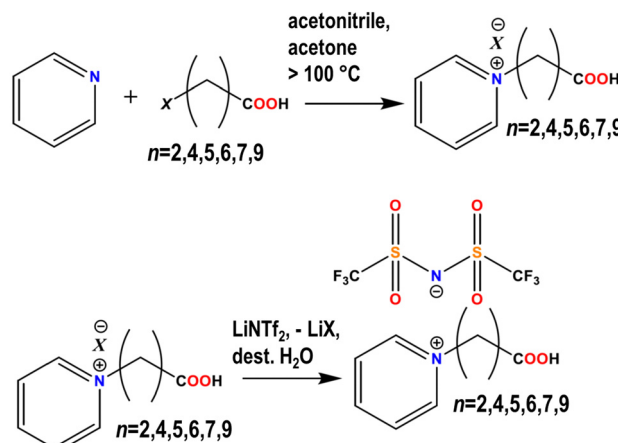
Scheme 1 Ionic liquids 1-(carboxyalkyl)pyridinium bis(trifluoromethylsulfonyl)imide $[\text{HOOC-(CH}_2\text{)}_n\text{-py}][\text{NTf}_2]$ with $n = 2, 4, 5, 6, 7, 9$ considered in this work. They comprise (A) carboxy-functionalized $(\text{HOOC-(CH}_2\text{)}_n\text{-py}^+)$ cations and (B) weakly interacting (NTf_2^-) anions; (C) it is expected that the structural motif of the doubly hydrogen bonded cationic dimers $(\text{HOOC-(CH}_2\text{)}_n\text{-py})_2$ is formed in these ILs. (D) Doubly H-bonded dimers of carboxylic acids represented by the molecular mimics of the IL cation.

solid state, the bulk liquid and even in the gaseous phase, although one anion was removed from (2,1) complexes.¹⁸

For understanding the nature of hydrogen bonding, in particular between ions of like charge, important questions arise, which will be properly addressed experimentally in the present study. How strong are the H-bonds between the two carboxy-functionalized cations compared to those between two neutral molecules in carboxylic acids? Are we able to further enhance the H-bond strength in the cationic dimers by increasing the alkyl chain length? What kind of influence does the variation of methylene groups have on the H-bond populations? Can we control the type and strength of H-bonds in liquids? The answers are of fundamental interest for understanding the nature of H-bonding between ions of like charge, not in ionic liquids only, but for similar H-bonds present in salt-bridges, peptides and DNA.

Synthesis of carboxy-functionalized ionic liquids

For addressing these fundamental issues, we synthesized and characterized carboxy-functionalized ILs n -(carboxyalkyl)pyridinium bis(trifluoromethylsulfonyl)imide $[\text{HOOC-(CH}_2\text{)}_n\text{-py}][\text{NTf}_2]$ with an increasing number of methylene groups CH_2 ($n = 2, 4, 5, 6, 7$, and 9) in two reaction steps as shown in Scheme 2. First, we prepared 1-(n -carboxyalkyl)pyridinium bromides with $n = 2, 4, 5, 6, 7$, and 9 as follows: pyridine was dissolved in acetonitrile and the solution was added dropwise to solid n -bromocarboxylic acids under vigorous stirring at 278 K. The resulting crystalline compounds were filtered and washed several times with acetonitrile and acetone. Then, they were dried under vacuum at 333 K and kept under argon. In the subsequent metathesis



Scheme 2 Reaction scheme for the synthesis of the ionic liquids 1-(carboxyalkyl)pyridinium bis(trifluoromethylsulfonyl)imide $[\text{HOOC-(CH}_2\text{)}_n\text{-py}][\text{NTf}_2]$ with $n = 2, 4, 5, 6, 7, 9$. X symbolizes the halogens Cl or Br.

reaction, equimolar amounts of lithium bis(trifluoromethylsulfonyl)imide and the n -(carboxyalkyl)pyridinium bromides were dissolved in water, resulting in an upper aqueous and a lower organic layer. The latter includes the 1-(n -carboxyalkyl)pyridinium bis(trifluoromethylsulfonyl)imide product and trace amounts of lithium bromide, which have been removed by washing several times with water. The residual amount of the Br-anion was determined using the reaction with silver nitrate. Finally, the samples were dried under vacuum at 333 K. The ILs $[\text{HOOC-(CH}_2\text{)}_n\text{-py}][\text{NTf}_2]$ with $n = 2, 4$ could be crystallized.¹⁸ (see also ESI I†) The recently published X-ray structures showed the characteristic double hydrogen bonding motif between the two carboxyl groups of the cations, despite the repulsive Coulomb forces between the positively charged pyridinium rings.¹⁸ In contrast, the weakly interacting bis(trifluoromethylsulfonyl)imide anions are not involved in hydrogen bonding with any of the cations in contrast to recently studied hydroxy-functionalized ILs.^{19–23} However, the newly synthesized ILs with $n = 5, 6, 7, 9$ could not be crystallized. Instead, the carboxy-functionalized ILs with longer alkyl chains $n > 4$ could be supercooled and finally formed glasses as given by the DSC thermograms in Fig. 1 (see also ESI III†). The glass transition temperatures could be reproduced for different heating and cooling rates and are around 220 K for all ILs.

Deuteron quadrupole coupling constants from solid-state deuterium NMR spectroscopy

The strength and distribution of the H-bond motifs present in the carboxy-functionalized ILs $[\text{HOOC-(CH}_2\text{)}_n\text{-py}][\text{NTf}_2]$ with $n = 2, 4, 5, 6, 7, 9$ were probed by solid-state deuterium NMR spectroscopy. For that purpose, hydrogen/deuterium (H/D) exchange was achieved by mixing the ILs with D_2O and removing water several times until nearly 100% deuteration was reached as proven by ^1H NMR. All samples have been dried under vacuum (3×10^{-3} mbar) for several days and the final water concentration (< 15 ppm) has been checked by Karl-Fischer titration.



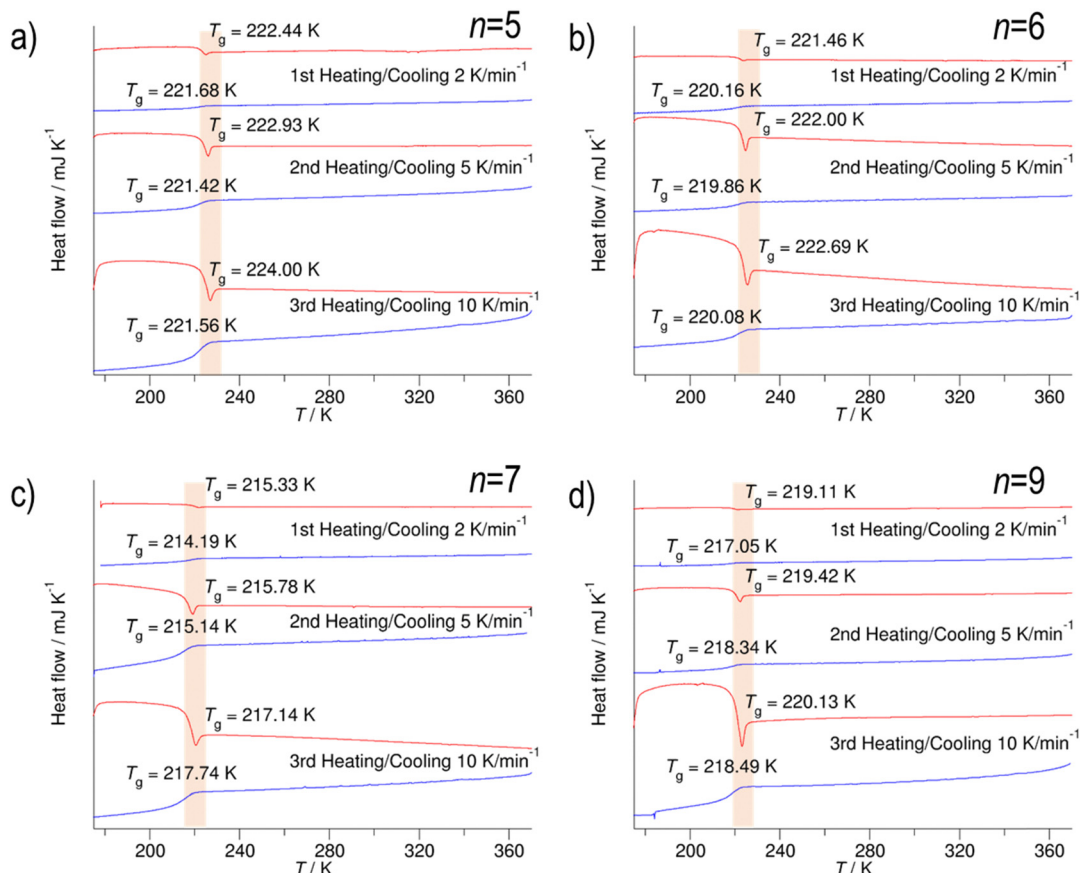


Fig. 1 The DSC thermograms of the ILs $[\text{HOOC-(CH}_2\text{)}_n\text{-py}][\text{NTf}_2]$ with (a) $n = 5$, (b) $n = 6$, (c) $n = 7$ and (d) $n = 9$, showing supercooling and finally glass transitions, indicated by the glass transition temperatures, T_g , between 215 and 220 K.

^2H NMR experiments were performed at Larmor frequency $\omega_2/2\pi = 61.42$ MHz on a Bruker Avance-400 spectrometer, using a high-power probe with a 5 mm horizontal solenoid coil. All ^2H NMR spectra were obtained by Fourier transformation of quadrature-detected phase-cycled quadrupole echo arising in the pulse sequence $(90_x^\circ - \tau_1 - 90_y^\circ - \tau_2 - \text{acquisition} - t)$, where $\tau_1 = 20$ μs , $\tau_2 = 21$ μs and t is a repetition time of the sequence during the accumulation of the NMR signal. The duration of the $\pi/2$ pulse was 1.6–1.7 μs . Spectra were typically obtained with 50–20 000 scans with the repetition time ranging from 0.5 to 15 seconds. To ensure reproducibility of the measurements, prior to each experimental investigation, the sealed glass ampule with the IL was placed in liquid nitrogen and then rapidly transferred to the pre-cooled NMR probe. The measured ^2H NMR spectra are shown in Fig. 2 for (a) ILs $n = 2, 4$, (b) ILs $n = 5, 6$ and (c) ILs $n = 7, 9$, respectively (see also ESI II[†]).

The ^2H NMR spectrum is characterized by two parameters: the quadrupole coupling constant DQCC, $\chi_D = (e^2 q_{zz} Q/h)$, and the asymmetry parameter, $\eta = q_{xx} - q_{yy}/q_{zz}$, which describes the principal elements q of the electric field gradient tensor.^{24–26} The DQCC is a measure of the magnitude of the electric field gradient at the deuterium site, while the asymmetry parameter provides information about the shape of the electric field gradient. For example, an asymmetry parameter of zero suggests a cylindrical

symmetry of the electric field gradient tensor along the O–D bond.²⁶ We determined the DQCCs from the solid-state deuterium NMR powder patterns for all carboxy-functionalized ILs with $n = 2, 4, 5, 6, 7$, and 9 for temperatures of 143 K and 203 K.

We obtained the DQCCs and the asymmetry parameters from a proper line shape analysis, providing two Pake patterns for all ILs with $n = 2, 4, 5, 6, 7, 9$.^{27,28} For the IL $[\text{HOOC-(CH}_2\text{)}_n\text{-py}][\text{NTf}_2]$ with the shortest alkyl chain length we obtained two values for the DQCC of 179 kHz and 208 kHz with asymmetry parameters $\eta = 0.12$ and $\eta = 0.13$, respectively (see Fig. 3). The small DQCC describes the OH···O=C H-bonds in the doubly hydrogen bonded cationic dimers ($\text{c}^+ = \text{c}^+$). This value is significantly smaller than about $\chi_D = 214\text{--}216$ kHz of the single OH···O H-bonds of D_2O ice,^{29,30} but in the order of DQCCs observed for carboxylic acids^{31,32} and salt bridges in proteins.³³ Obviously, two strong cooperative H-bonds easily overcome the repulsive Coulomb forces between the two cations. The larger DQCC is assigned to the single OH···O=S H-bonds between the cation and the anion in the ($\text{c}^+ - \text{c}^- - \text{a}^-$) complexes (see Scheme 3). This value agrees with the reported DQCC for the Coulomb-enhanced ($\text{c}^+ - \text{a}^-$) H-bonds in hydroxy-functionalized ILs.³⁴ The asymmetry parameters η for both types of H-bonds range between 0.1 and 0.13, typical values for deuterons involved in linear OH···O H-bonds as observed for water and

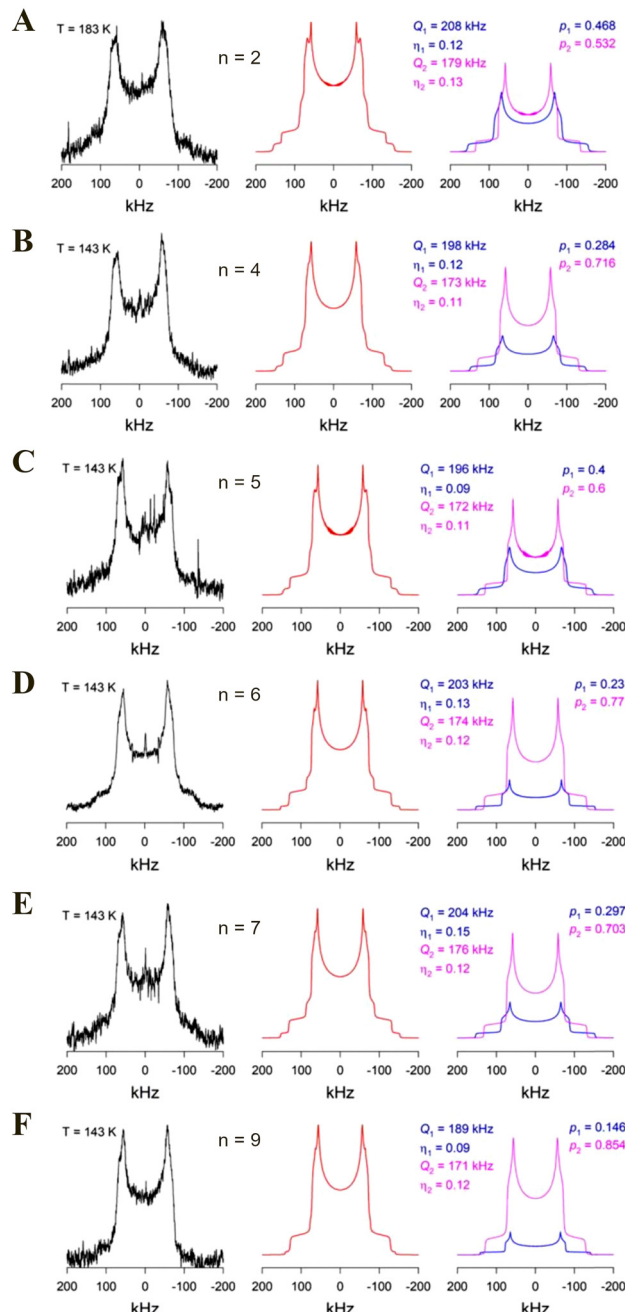


Fig. 2 (A) ^2H NMR spectrum at 183 K and line shape analysis for carboxy-functionalized ionic liquids $[\text{DOOC-(CH}_2)_n\text{-Py}][\text{NTf}_2]$ with $n = 2$. (B) ^2H NMR spectrum at 143 K and line shape analysis for carboxy-functionalized ionic liquids $[\text{DOOC-(CH}_2)_n\text{-Py}][\text{NTf}_2]$ with $n = 4$. (C) ^2H NMR spectrum at 143 K and line shape analysis for carboxy-functionalized ionic liquids $[\text{DOOC-(CH}_2)_n\text{-Py}][\text{NTf}_2]$ with $n = 5$. (D) ^2H NMR spectrum at 143 K and line shape analysis for carboxy-functionalized ionic liquids $[\text{DOOC-(CH}_2)_n\text{-Py}][\text{NTf}_2]$ with $n = 6$. (E) ^2H NMR spectrum at 143 K and line shape analysis for carboxy-functionalized ionic liquids $[\text{DOOC-(CH}_2)_n\text{-Py}][\text{NTf}_2]$ with $n = 7$. (F) ^2H NMR spectrum at 143 K and line shape analysis for carboxy-functionalized ionic liquids $[\text{DOOC-(CH}_2)_n\text{-Py}][\text{NTf}_2]$ with $n = 9$. Experimental spectra are shown with black lines, simulated spectra are shown with red lines and deconvoluted simulated spectra are shown with blue and pink lines (specie 1 and specie 2 correspondingly). Q denote the DQCCs, η the asymmetry parameters, and p the relative populations (fractions) of the $(\text{c}^+=\text{c}^+)$ and $(\text{c}^+-\text{c}^+-\text{a}^-)$ bound species. Number 1 is referred to $(\text{c}^+-\text{c}^+-\text{a}^-)$, and number 2 to $(\text{c}^+=\text{c}^+)$ H-bonded cations and anions.

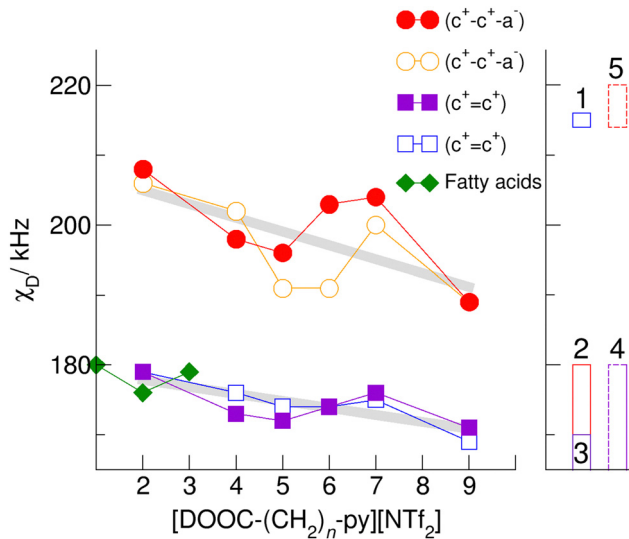
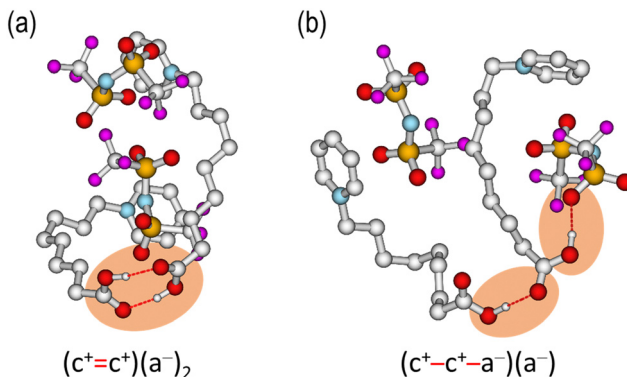


Fig. 3 (a) Measured and deconvoluted DQCCs of carboxy-functionalized ionic liquids $[\text{DOOC-(CH}_2)_n\text{-Py}][\text{NTf}_2]$ with $n = 2, 4, 5, 6, 7, 9$ for temperatures 143 K (closed symbols) and 203 K (open symbols), respectively. The DQCCs for the (c^+-a^-) H-bonds (open symbols) decrease from 210 kHz down to 190 MHz with increasing number of methylene groups. Due to the strong double H-bonds in the cationic dimers ($\text{c}^+=\text{c}^+$), the DQCCs are lower but also decrease with the same trend from 180 kHz down to 170 kHz. We also added the measured DQCC for doubly H-bonded dimers ($\text{m}=\text{m}$) of phenylacetic acid, phenylpropanoic acid and phenylbutanoic acids, representing molecular mimics of the carboxy-functionalized cations in the ILs. (b) For comparison we show the DQCCs for D₂O ice (1),^{29,30} carboxylic acids (2),^{31,32} salt bridges in proteins (3)³³ as well as for (c^+-c^+) (4) and (c^+-a^-) (5) H-bonds in hydroxy-functionalized ILs.³⁴

alcohols.³⁰ With increasing alkyl chain length n , in the cationic dimers ($\text{c}^+=\text{c}^+$) the DQCC decreases from 179 kHz to 169 kHz, indicating stronger H-bonding caused by reduced Coulomb repulsion between the positively charged rings in the cations. Similar is observed for the DQCCs in the OH \cdots O=S H-bonds between the cation and the anion in the $(\text{c}^+-\text{c}^+-\text{a}^-)$ complexes. The (c^+-a^-) H-bonds are enhanced due to weaker repulsive forces between the neighboring cations. This observation also underlines, why we do not consider the regular Coulomb enhanced H-bonds within isolated (c^+-a^-) ion pairs: in such case, a larger size of the alkyl spacer would decrease the Coulombic attraction within the pair and thus decrease the H-bonds strength, leading to higher DQCC values. Observation of the opposite trend indicates that no individual (c^+-a^-) ion pairs exist, in favor of $(\text{c}^+-\text{c}^+-\text{a}^-)$ complexes. We know from recent IR experiments that $(\text{c}^+=\text{c}^+)$ bonds are stronger than (c^+-a^-) H-bonds resulting in significant redshifts of the CO IR stretching frequencies.¹⁸ Thus, we conclude that the larger DQCCs of about 200 kHz are related to Coulomb enhanced (c^+-a^-) ion pairs, whereas the smaller DQCC of about 180 kHz characterizes the $(\text{c}^+=\text{c}^+)$ interaction in cationic dimers. The asymmetry parameters stay almost the same with n and only slightly decrease as expected for stronger H-bonds towards $n=9$ (see Figure S2, ESI[†]). Several references in the literature discussed a linear dependence between proton chemical shifts, $\delta^1\text{H}$, and deuteron quadrupole coupling constants, DQCCs, for



Scheme 3 Calculated locally stable H-bond motifs $(c^+ = c^+)(a^-)_2$ and $(c^+ - c^+ - a^-)(a^-)$ of the neutral quaternary complexes for the ILs 1-(carboxyethyl)pyridinium bis(trifluoromethylsulfonyl)imide $[\text{HOOC}-(\text{CH}_2)_8-\text{py}]\text{[NTf}_2]$ resembling the binding situation in the IL $[\text{HOOC}-(\text{CH}_2)_8-\text{py}]\text{[NTf}_2]$. (a) The structural motif includes the doubly H-bonded cations $(c^+ = c^+)$. (b) In the open structures, the ring motif of the doubly H-bonded cations $(c^+ = c^+)$ is opened and replaced by an H-bond complex $(c^+ - c^+ - a^-)$ with one remaining H-bond $(c^+ - c^+)$ and an additional H-bond $(c^+ - a^-)$ between the cation and anion.

N-H/D and O-H/D functional groups in molecular and ionic liquids, supporting the role of DQCCs as sensitive probes of hydrogen bonding.^{35,36}

Now we turn to the question of whether the double H-bonds in the cationic dimers ($c^+ = c^+$) are weaker than those in molecular dimers ($m = m$)? For this purpose, we measured the DQCC values for phenylacetic acid, phenylpropanoic acid and phenylbutanoic acids. These molecules are the structural analogues to the cations of the investigated ILs. The positively charged pyridinium ring is simply replaced by a phenyl ring. DQCCs of 180 kHz, 176 kHz and 179 kHz were measured for the compounds at room temperature, which are only slightly higher than those observed at lower temperatures for the corresponding carboxy-functionalized ILs (see Figure S3, ESI[†]). Obviously, the Coulomb repulsion between the two polarizable pyridinium rings is fully compensated by the attractive interaction with the NTf_2^- counterions, resulting in equally strong ($c^+ = c^+$) and ($m = m$) H-bonds. As we have seen, this effect is only moderately enhanced by lengthening the alkyl chain. We can thus show for the first time that ($c^+ = c^+$) H-bonds in cationic dimers can be as strong as those between two neutral molecules. A suitable physical and chemical environment, in this case polarizable cations and weakly interacting anions, creates a molecular island on which H-bonds can form perfectly and Coulomb repulsion plays no role.

The assignment and interpretation of the DQCCs and asymmetry parameters is confirmed by calculating $(c^+ = c^+)(a^-)_2$ and $(c^+ - c^+ - a^-)(a^-)$ H-bonded complexes of the ILs along with doubly H-bonded dimers ($m = m$) of the molecular mimics of the IL cations at the B3LYP-D3/6-31+G* level of theory. The resulting structures and H-bond motifs are shown in the ESI[†] and resemble those of the two complexes presented for the IL $[\text{HOOC}-(\text{CH}_2)_8-\text{py}]\text{[NTf}_2]$ in Scheme 3.³⁷⁻⁴⁰ The differences between the calculated DQCCs obtained for the $(c^+ = c^+)(a^-)_2$

and $(c^+ - c^+ - a^-)(a^-)$ H-bond motifs range between 15 and 30 kHz and agree with the measured differences, finally supporting our interpretation. Moreover, the calculated DQCCs for phenylacetic acid, phenylpropanoic acid and phenylbutanoic acid ($m = m$) dimers are almost equal to the DQCCs obtained for the $(c^+ = c^+)(a^-)_2$ IL complexes, confirming that the $(c^+ = c^+)$ H-bonds and ($m = m$) H-bonds are of similar strength, despite the Coulomb repulsion between the cations (see also ESI IV and V[†]).

Populations of $(c^+ - a^-)$ and $(c^+ = c^+)$ clusters from solid-state deuterium NMR

NMR solid-state spectra measured in the crystalline or glassy state provide quantitative information about the populations of the local H-bond arrangements present in the ILs. In Fig. 4, we show the populations q_1 of $(c^+ - a^-)$ H-bonds and q_2 of $(c^+ = c^+)$ H-bonds in carboxy-functionalized ionic liquids $[\text{DOOC}-(\text{CH}_2)_n-\text{py}]\text{[NTf}_2]$ with $n = 2, 4, 5, 6, 7$, and 9, determined at 143 K and 203 K. In the IL $[\text{DOOC}-(\text{CH}_2)_2-\text{py}]\text{[NTf}_2]$ the two types of H-bonds are almost present in equal amounts. We find $q_1 = 0.55$ for $(c^+ - a^-)$ H-bonds and $q_2 = 0.45$ for $(c^+ = c^+)$ H-bonds, respectively. We now clarify how the propensity for the formation of $(c^+ = c^+)$ H-bonds depends on the alkyl chain length between two cationic rings and their COOH groups. With increasing alkyl chain length, the population q_1 of the $(c^+ - a^-)$ H-bonds decreases from 0.55 for $n = 2$, via 0.30 for $n = 5$ down to 0.10 for $n = 9$ for the benefit of increasing amounts of $(c^+ = c^+)$ H-bonds.

The increase of the $(c^+ = c^+)$ H-bonds correlates with the lowering of the corresponding DQCCs. For $n = 9$, the H-bond population is almost solely dominated by cationic dimers ($c^+ = c^+$). Obviously, cooperative H-bond attraction is not only able to compensate for the repulsive Coulomb forces but also

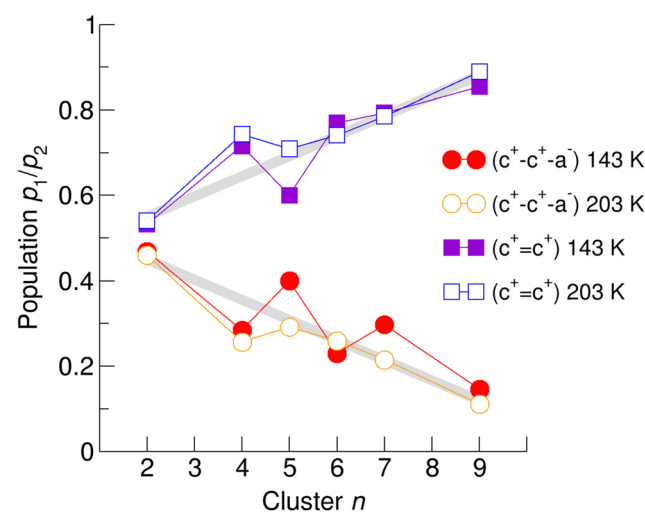


Fig. 4 Populations q_1 of $(c^+ - a^-)$ H-bonds and q_2 of $(c^+ = c^+)$ H-bonds in carboxy-functionalized ionic liquids $[\text{DOOC}-(\text{CH}_2)_n-\text{py}]\text{[NTf}_2]$ with $n = 2, 4, 5, 6, 7$, and 9, derived from NMR solid-state spectra at 143 K (open symbols) and 203 K (closed symbols). At $n = 9$, the population is almost solely governed by $(c^+ = c^+)$ H-bonds.

able to ignore the H-bond accepting capabilities of the counter anion completely. In this regard, we provide the first evidence for quasi-isolated cationic dimers in solution that are stabilized by strong and directional H-bonds.

Conclusion

We synthesized and characterized carboxy-functionalized ionic liquids $[\text{DOOC-(CH}_2\text{)}_n\text{-py}][\text{NTf}_2]$ with an increasing number of methylene groups $n = 2, 4, 5, 6, 7$, and 9 for controlling the Coulomb repulsion between the cations and fostering the formation of doubly H-bonded cationic ($\text{c}^+ = \text{c}^+$) dimers, resembling the archetype of H-bonding in formic acid. We then measured DQCCs and population of ($\text{c}^+ - \text{a}^-$) H-bonds and ($\text{c}^+ = \text{c}^+$) H-bonds in the crystalline and glassy states of the ILs by means of ^2H NMR solid-state spectroscopy. We observed two Pake patterns for deuterons involved in ($\text{c}^+ - \text{a}^-$) H-bonds and ($\text{c}^+ = \text{c}^+$) H-bonds, respectively. The DQCCs of deuterons in the ($\text{c}^+ = \text{c}^+$) H-bonds are about 15–30 kHz smaller than those in ($\text{c}^+ - \text{a}^-$) H-bonds, indicating stronger H-bonds despite repulsive Coulomb forces in the first and attractive ones in the latter case. As expected, ($\text{c}^+ = \text{c}^+$) H-bonds increase with longer alkyl chains and finally dominate the H-bond populations solely. Apparently, the cooperative H-bonding is not only able to compensate the repulsive Coulomb forces but also to completely ignore the H-bond accepting abilities of the counter anion. In this context, we provide the first evidence for quasi-isolated cationic dimers in solution stabilized by strong and directional H-bonding. We also measured the DQCCs of phenylacetic acid, phenylpropanoic acid and phenylbutanoic acids, representing the molecular analogues of the IL cations for $n = 1, 2$, and 3 . Their DQCCs were almost similar to those observed for the carboxy-functionalized ILs, indicating equally strong ($\text{c}^+ = \text{c}^+$) and ($\text{m} = \text{m}$) H-bonds. This opens up the prospect of being able to detect the first isolated cationic dimer, in which the ions of like charge are held together by two strong hydrogen bonds despite the repulsive Coulomb interaction between them.

Data availability

The data will be available upon request to the authors.

Conflicts of interest

There are no conflicts to declare.

Acknowledgements

This work was supported by the Russian Science Foundation (grant No. 24-13-00129) and by DFG Research Grants LU-506/17-1, project no. 470038970 and LU-506/18-1, and project no. 517661181.

References

- 1 G. A. Jeffrey and W. Saenger, *Hydrogen Bonding in Biological Structures*, Springer, Berlin, 1991.
- 2 J. H. Hoeijmakers, *N. Engl. J. Med.*, 2009, **361**, 1475–1485.
- 3 R. Kalescky, E. Kraka and D. Cremer, Accurate determination of the binding energy of the formic acid dimer: The importance of geometry relaxation, *J. Chem. Phys.*, 2014, **140**, 084315.
- 4 F. Kollipost, R. W. Larsen, A. V. Domanskaya, M. Nörenberg and M. A. Suhm, The highest frequency hydrogen bond vibration and an experimental value for the dissociation energy of formic acid dimer, *J. Chem. Phys.*, 2012, **136**, 151101.
- 5 Z. Xue and M. A. Suhm, Adding more weight to a molecular recognition unit: the low-frequency modes of carboxylic acid dimers, *Mol. Phys.*, 2010, **108**, 2279–2288.
- 6 M. Allan, Electron Collisions with Formic Acid Monomer and Dimer, *Phys. Rev. Lett.*, 2007, **98**, 123201.
- 7 P. McMullen, Q. Qiao, S. Luozhong, L. Cai, L. Fang, Q. Shao and S. Jiang, Motif-based zwitterionic peptides impact their structure and immunogenicity, *Chem. Sci.*, 2022, **13**, 10961–10970.
- 8 H. Weingärtner, Understanding Ionic Liquids at the Molecular Level: Facts, Problems, and Controversies, *Angew. Chem., Int. Ed.*, 2008, **47**, 654–670.
- 9 N. V. Plechkova and K. R. Seddon, Applications of ionic liquids in the chemical industry, *Chem. Soc. Rev.*, 2008, **37**, 123–150.
- 10 K. Fumino, T. Peppel, M. Geppert-Rybczynska, D. H. Zaitsau, J. K. Lehmann, S. P. Verevkin, M. Köckerling and R. Ludwig, The influence of hydrogen bonding on the physical properties of ionic liquids, *Phys. Chem. Chem. Phys.*, 2011, **13**, 14064–14075.
- 11 P. A. Hunt, C. R. Ashworth and R. P. Matthews, Hydrogen bonding in ionic liquids, *Chem. Soc. Rev.*, 2015, **44**, 1257–1288.
- 12 S. Scheiner, Assessment of the Presence and Strength of H-Bonds by Means of Corrected NMR, *Molecules*, 2016, **21**, 1426.
- 13 I. Alkorta, I. Mata, E. Molins and E. Espinosa, Charged versus Neutral Hydrogen-Bonded Complexes: Is There a Difference in the Nature of the Hydrogen Bonds?, *Chem. – Eur. J.*, 2016, **22**, 9226–9234.
- 14 I. Mata, E. Alkorta and E. Molins, Espinosa, Electrostatics at the Origin of the Stability of Phosphate-Phosphate Complexes Locked by Hydrogen Bonds, *Chem. Phys. Chem.*, 2012, **13**, 1421–1424.
- 15 I. Mata, I. Alkorta, E. Molins and E. Espinosa, Tracing environment effects that influence the stability of anion-anion complexes: The case of phosphate–phosphate interactions, *Chem. Phys. Lett.*, 2013, **555**, 106–109.
- 16 (a) F. Weinhold and R. A. Klein, Anti-Electrostatic Hydrogen Bonds, *Angew. Chem., Int. Ed.*, 2014, **53**, 11214–11217; (b) Corrigendum: F. Weinhold and R. A. Klein, *Angew. Chem., Int. Ed.*, 2014, **53**, 12992.
- 17 L. Hunger, L. Al-Sheakh, D. Zaitsau, S. P. Verevkin, A. Appelhagen, A. Villinger and R. Ludwig, Dissecting Noncovalent



Interactions in Carboxyl-Functionalized Ionic Liquids Exhibiting Double and Single Hydrogens Bonds Between Ions of Like Charge, *Chem. – Eur. J.*, 2022, **28**(46), e202200949.

18 L. Hunger, L. Al Sheakh, S. Fritsch, A. Villinger, R. Ludwig, P. Harville, O. Moss, A. Lachowicz and M. A. Johnson, Spectroscopic Evidence for Doubly Hydrogen-Bonded Cationic Dimers in the Solid, Liquid, and Gaseous Phases of Carboxyl-Functionalized Ionic Liquids, *J. Phys. Chem. B*, 2024, **128**, 5463–5471.

19 A. Knorr, K. Fumino, A.-M. Bonsa and R. Ludwig, Spectroscopic evidence of ‘jumping and pecking’ of cholinium and H-bond enhanced cation–cation interaction in ionic liquids, *Phys. Chem. Chem. Phys.*, 2015, **17**, 30978–30982.

20 A. Knorr and R. Ludwig, Cation–cation clusters in ionic liquids: Cooperative hydrogen bonding overcomes like-charge repulsion, *Sci. Rep.*, 2015, **5**, 17505.

21 A. Knorr, P. Stange, K. Fumino, F. Weinhold and R. Ludwig, Spectroscopic Evidence for Clusters of Like-Charged Ions in Ionic Liquids Stabilized by Cooperative Hydrogen Bonding, *Chem. Phys. Chem.*, 2016, **17**, 458–462.

22 A. Strate, T. Niemann, D. Michalik and R. Ludwig, When Like Charged Ions Attract in Ionic Liquids: Controlling the Formation of Cationic Clusters by the Interaction Strength of the Counterions, *Angew. Chem., Int. Ed.*, 2017, **56**, 496–500.

23 F. S. Menges, H. J. Zeng, P. J. Kelleher, O. Gorlova, M. A. Johnson, T. Niemann, A. Strate and R. Ludwig, Structural Motifs in Cold Ternary Ion Complexes of Hydroxyl-Functionalized Ionic Liquids: Isolating the Role of Cation–Cation Interactions, *J. Phys. Chem. Lett.*, 2018, **9**, 2979–2984.

24 H. Huber, Deuterium quadrupole coupling constants. A theoretical investigation, *J. Chem. Phys.*, 1985, **83**, 4591–4598.

25 R. Eggenberger, S. Gerber, H. Huber, D. Searles and M. Welker, Ab initio calculation of the deuterium quadrupole coupling in liquid water, *J. Chem. Phys.*, 1992, **97**, 5898–5904.

26 P. L. Cummins, G. B. Bacskey, N. S. Hush, B. Halle and S. Engström, The effect of intermolecular interactions on the 2H and 17O quadrupole coupling constants in ice and liquid water, *J. Chem. Phys.*, 1985, **82**, 2002–2013.

27 J. G. Powles and J. H. Strange, Zero Time Resolution Nuclear Magnetic Resonance Transient in Solids, *Proc. Phys. Soc., London*, 1963, **82**, 6–15.

28 G. E. Pake, Nuclear resonance absorption in hydrated crystals: fine structure of the proton line, *J. Chem. Phys.*, 1948, **16**, 327–336.

29 D. T. Emonds and A. L. Mackay, The pure quadrupole resonance of the deuteron in ice, *J. Magn. Reson.*, 1975, **20**, 515–519.

30 T. V. Krivokhzhina and R. J. Wittebort, 2Q NMR of $2\text{H}_2\text{O}$ ordering at solid interfaces, *J. Magn. Reson.*, 2014, **243**, 33–39.

31 X. Shi and C. M. Rienstra, Site-Specific Internal Motions in GB1 Protein Microcrystals Revealed by $3\text{D}^2\text{H}-^{13}\text{C}-^{13}\text{C}$ Solid-State NMR Spectroscopy, *J. Am. Chem. Soc.*, 2016, **138**, 4105–4119.

32 J. W. Clymer and J. L. Ragle, Deuterium quadrupole coupling in methanol, salicyclic acid, catechol, resorcinol, and hydroquinone, *J. Chem. Phys.*, 1982, **77**, 4366–4373.

33 J. M. Jackman, J. C. Trewella and R. C. Haddon, Studies in nuclear magnetic resonance spectroscopy. 17. Deuteron quadrupole coupling constants in intramolecularly hydrogen bonded systems, *J. Am. Chem. Soc.*, 1980, **102**, 2519–2525.

34 A. E. Khudozhitkov, V. Overbeck, P. Stange, D. Paschek, A. G. Stepanov, D. I. Kolokolov and R. Ludwig, Hydrogen Bonding Between Ions of Like Charge in Ionic Liquids Characterized by NMR Deuteron Quadrupole Coupling Constants—Comparison with Salt Bridges and Molecular Systems, *Angew. Chem., Int. Ed.*, 2019, **58**, 17863–17871.

35 M. Strauch, A.-M. Bonsa, B. Golub, V. Overbeck, D. Michalik, D. Paschek and R. Ludwig, Deuteron Quadrupole Coupling Constants and Reorientational Correlation Times in Protic Ionic Liquids, *Phys. Chem. Chem. Phys.*, 2016, **18**, 17788–17794.

36 A. Strate, V. Overbeck, V. Lehde, J. Neumann, A.-M. Bonsa, T. Niemann, D. Paschek, D. Michalik and R. Ludwig, The Influence of Like-Charge Attraction on the Structure and Dynamics of Ionic Liquids: NMR Chemical Shifts, Quadrupole Coupling Constants, Rotational Correlation Times and Failure of Stokes-Einstein-Debye, *Phys. Chem. Chem. Phys.*, 2018, **20**, 5617–5625.

37 M. J. Frisch, G. W. Trucks, H. B. Schlegel, G. E. Scuseria, M. A. Robb, J. R. Cheeseman, G. Scalmani, V. Barone, G. A. Petersson, H. Nakatsuji, X. Li, M. Caricato, A. Marenich, J. Bloino, B. G. Janesko, R. Gomperts, B. Mennucci, H. P. Hratchian, J. V. Ortiz, A. F. Izmaylov, J. L. Sonnenberg, D. Williams-Young, F. Ding, F. Lipparini, F. Egidi, J. Goings, B. Peng, A. Petrone, T. Henderson, D. Ranasinghe, V. G. Zakrzewski, J. Gao, N. Rega, G. Zheng, W. Liang, M. Hada, M. Ehara, K. Toyota, R. Fukuda, J. Hasegawa, M. Ishida, T. Nakajima, Y. Honda, O. Kitao, H. Nakai, T. Vreven, K. Throssell, J. A. Montgomery Jr., J. E. Peralta, F. Ogliaro, M. Bearpark, J. J. Heyd, E. Brothers, K. N. Kudin, V. N. Staroverov, T. Keith, R. Kobayashi, J. Normand, K. Raghavachari, A. Rendell, J. C. Burant, S. S. Iyengar, J. Tomasi, M. Cossi, J. M. Millam, M. Klene, C. Adamo, R. Cammi, J. W. Ochterski, R. L. Martin, K. Morokuma, O. Farkas, J. B. Foresman and D. J. Fox, *Gaussian 09, Revision A.02*, Gaussian, Inc., Wallingford CT, 2016.

38 S. Grimme, J. Antony, S. Ehrlich and H. Krieg, A consistent and accurate ab initio parametrization of density functional dispersion correction (DFT-D) for the 94 elements H–Pu, *J. Chem. Phys.*, 2010, **132**, 154104.

39 S. Ehrlich, J. Moellmann, W. Reckien, T. Bredow and S. Grimme, System-Dependent Dispersion Coefficients for the DFT-D3 Treatment of Adsorption Processes on Ionic Surfaces, *Chem. Phys. Chem.*, 2011, **12**, 3414–3420.

40 S. Grimme, A. Jansen, J. G. Brandenburg and C. Bannwarth, Dispersion-Corrected Mean-Field Electronic Structure Methods, *Chem. Rev.*, 2016, **116**, 5105–5154.

